DAC Vacuum Moisture Swing

Initial Design Report

Randy Brierley: Automation and Controls / Website Lead
Justin Patterson: Lab Quality / Project Manager
Branden Welker: Ansys Expert / Fundraising Lead
Elijah Woolridge: Modeling Lead / Budget Manager

Fall 2025-Spring 2026

Project Sponsor: Salt River Project
Faculty Advisor: Professor Jennifer Wade
Sponsor Mentor: PHD Candidate Stephano Sinyangwe
Instructor: Professor David Willy

DISCLAIMER

This report was prepared by students as part of a university course requirement. While considerable effort has been put into the project, it is not the work of licensed engineers and has not undergone the extensive verification that is common in the profession. The information, data, conclusions, and content of this report should not be relied on or utilized without thorough, independent testing and verification. University faculty members may have been associated with this project as advisors, sponsors, or course instructors, but as such they are not responsible for the accuracy of results or conclusions.

EXECUTIVE SUMMARY

The goal of this project is to design and build a direct air capture device that utilizes a vacuum moisture swing process to separate CO2 from ambient air. This process utilizes common sorbent materials to bind to CO2 as air passes through them, and then it leverages a process in which moisture unbinds the CO2 from the sorbents. The intent is to have a scalable design which will be practical and energy-efficient for large-scale deployment near high CO2 areas such as factories.

The project's client is Dr. Wade, who has been developing the vacuum moisture process in NAU's Climate Solutions Lab. It is sponsored by SRP, who is providing the bulk of the funding. The project is being completed under the requirements of the ME476C class.

The project has two primary goals: to design a structured sorbent bed that will be more energy efficient than the standard packed bed, and to build a functioning, lab-scale device which will perform the vacuum moisture swing process. The structured sorbent beds will be designed as CAD models and run through CFD simulations to optimize their structures. The device will be designed to run the full direct air capture cycle, with most aspects automated.

The device will run through a five step cycle: adsorption, evacuation, desorption, final evacuation, and pressurization. During adsorption, ambient air will be pulled through the sorbent bed. The sorbent bed will then be isolated from atmosphere and a vacuum pump will draw down to complete evacuation. A water reservoir will then be exposed, causing the water to vaporize and unbind the CO2 from the sorbents in the desorption stage. The water reservoir will then be isolated and a final draw-down of the sorbent chamber will complete the final evacuation. Finally the sorbent bed will be exposed to ambient pressure, which will pressurize the system. The system can then repeat the cycles.

The new designs of the structured sorbent beds are intended to provide a lower resistance to flow, thereby decreasing the power requirement to run the cycle. A primary intent of this project is as a proof-of-concept that a vacuum moisture swing process can be a viable option for removing CO2 from air in large-scale, real-world applications.

As of writing this document, the design is still in development. Initial CFD simulations have begun. A process diagram has been fully fleshed out. A 3D printer has been selected. The next stages are selecting specific model parts for all aspects of the system, testing different sorbent structures, and creating the control architecture for the device.

TABLE OF CONTENTS

Contents

1 BACKGROUND

This chapter contains a project description, deliverables, and success metrics. The project description gives an overview of the project, sponsors, and the importance of the project. The deliverables section discusses the deliverables based on the client, the course, and the team's goals. Success metrics are described for the primary aspects of the projects, and the methods of gauging success are discussed.

1.1 Project Description

The goal of this project is to create a direct air capture device which utilizes a vacuum moisture swing technique to extract CO2 from air. The CO2 capture will be achieved by a sorbent bed, with structured sorbent beds developed and tested against the performance of a packed bed. The vacuum moisture swing device will function by pushing air through the sorbent bed, resulting in cleaner air exiting. A vacuum will then be pulled, which will cause a reservoir of water at room temperature to vaporize. The water vapor will be pulled through the sorbent bed, causing the CO2 to unbind from sorbent. The CO2 will be carried downstream and contained. The cycle will then repeat.

The dynamics of the vacuum moisture swing process have already been calculated and simulated by the NAU Climate Solutions Lab, and will inform many of the parameters of the cycle. For this project, the team will focus on optimizing the sorbent bed and designing a functioning and automated vacuum moisture swing DAC device.

The project's client is Dr. Jennifer Wade. SRP is sponsoring the project, and have promised $50,000. The NAU Green Fund has been applied to for $2000 and is awaiting approval. Based on early budgeting, this total will be more than sufficient for completing the full project.

This project is important as a proof-of-concept of a novel method of removing CO2 from air. CO2 is the largest contributor to global warming and ocean acidification. The client intends for the design to be scaled up in the future to provide a method of extracting CO2 from the air near factories. If the vacuum moisture swing design proves to be effective and energy efficient, it could be deployed near many factories and other CO2-producing facilities and significantly decrease CO2 emissions.

1.2 Deliverables

The two primary deliverables for the client are structured sorbent beds and a vacuum moisture swing device. The structured sorbent beds must perform better than a standard packed sorbent bed. The vacuum moisture swing device must be capable of testing a wide range of sorbent beds while maintaining the temperature and speed conditions that the client has specified. Further deliverables for the device are that it must be automated, maintain a clean lab environment, and output the data to Matlab.

The ME476C course deliverables are to complete three presentations, two reports, several individual learning assignments, and weekly timecards and staff meetings. In addition, the team has set client deliverables of meeting with the mentor every week and the client biweekly.

1.3 Success Metrics

Success for this project will be based on two categories: the structured sorbent beds and the vacuum moisture swing device. Success in the structured sorbent beds will be assessed by creating one which performs better than the baseline of a packed sorbent bed. The proposed designs will have computational fluid dynamics performed with ANSYS to simulate airflow through them. Designs successful in simulation will then be tested in the vacuum moisture swing device. Success of these structures will be analyzed by observing the pressure drop, and the adsorption efficiency, based on pressure transducers and gas analyzers. The pressure drop must be lower than the packed bed, and the adsorption capacity must be reasonably close to the packed bed. Testing will therefore include a packed bed to obtain the baseline numbers which will be used to analyze success of the structured beds.

Success in the vacuum moisture swing device will be based on whether it can create and maintain the conditions desired for the vacuum swing process. Calculations will be performed to identify the ideal velocity and pressure during the adsorption and desorption processes. The client has already identified the steps in the cycle (being adsorption, evacuation, desorption, final evacuation, and pressurization). The device must cycle through these steps properly, opening and closing valves, powering on and off pumps and heating elements, and recording data from sensors throughout the process. If the device can perform the full vacuum moisture swing cycle on all of the sorbents that are tested, it will be a success.

2 REQUIREMENTS

This chapter contains customer requirements, engineering requirements, and House of Quality. The customer requirements are listed out and the metrics for each are given. The engineering requirements are listed and the quantifiable targets are given for each. A House of Quality which compares different sorbent beds is shown, along with a discussion of the process through which it was arrived at.

2.1 Customer Requirements (CRs)

Capture as much CO2 as possible

- *Measured as kg of CO2 delivered at output per hour (RANDOM EXAMPLEs SOMEONE VERIFY PLEASE, thanks)*

2. *Minimize power requirement*
    - *Measured as the average KW/h consumed for a standard cycle.*
3. *Utilize moisture swing*
    - *A novel carbon capture process in which the absorption and release of CO2 is controlled by relative humidity.*
4. *Minimize water loss*
    - *Defined as the mass of non-reclaimable water consumed by the system.*
5. *Track the metrics of the apparatus as it runs*
    - *Sensors are requested for before and after the sorbent bed.*
6. *Be able to control flow rate and pressure*
    - *Through the sorbent bed and in the vacuum boiler respectively*
7. *Maintain clean lab environment by using an oil-free vacuum pump*
    - *This prevents contamination of the output water and gas.*
8. *Keep design compact*
    - *The design must be a practical scale for small batch tests of experimental sorbents and fit within the available lab space.*
9. *Utilize existing common vacuum parts*
    - *To keep costs down, save time, and allow for future modifications or scaling.*

2.2 Engineering Requirements (ERs)

1a. Maximize sorbent productivity [(mmol CO2/g sorbent)/hour]

1b. Maximize packing density (cm^3/cm^3)

1c. Find ideal void fraction (cm^3/c^3)

2a. Minimise pressure drop (ΔkPa/cm)

2b. Keep air velocity within practical range, <1m/s

3a. Vacuum pressure below water vaporization pressure at ambient temperature, <~3kPa

4a. Reuse water by condensing water vapor (°C)

4b. Heat water reservoir to offset evaporative cooling to maintain ambient temperature (~15 °C)

5a. Incorporate pressure transducers before and after reactor chamber (kPa)

5b. Incorporate thermocouples before and after reactor chamber (°C)

6a. Incorporate a VFD (matched to vacuum pump, rated by kW)

6b. Incorporate control logic (most likely a PLC, possibly analogue feedback from 4-20mA sensors)

2.3 House of Quality (HoQ)

Once the customer and engineering requirements were determined a house of quality was created to set goals and determine the most important design factors. The house of quality can be seen in figure x.

						0							
					0	0							
				0	0	+							
			0	0	0	+							
		+	0	0	0	+							
	0	-	0	0	0	+							
-	-	-	0	0	+	+							
+	-	-	+	-	+	+	+						

weight	Customer Requirements	Sorbent Efficiency	Packing Density	Pressure Drop	Practical Velocity Range	Vacuum Pressures	Condensor	Sensor Integration	PLC	VFD	Packed Bed	Monolithic	Laminate
25	C02 Capture Effeciency	5	3.5	2	2.5	3	2	3	3	2	5	2	3
22.5	Minimal Power Input	1.5	2.5	4.5	3	3.5	2	2.5	3	4	1	5	4
7.5	Vaporization Without Heating	1	1.5	2	2	4.5	1.5	1.5	1.5	2	2	5	3
32.5	Measurable Results	1.5	1.5	1	2	1.5	1.5	5	2.5	1.5	2	5	4
12.5	Controllable Flow Rate	1	1.5	2	2.5	2	1.5	5	5	4.5	2	5	4
Units		mmol/gm	^3/m^	kPa	m/s	kPa	QTY	QTY	QTY	QTY			
Target Score		>1.5	>0.6	<0.5	<1	<3	1	6	1	1			
Relative Importance Weight		2.275	2.225	2.2375	2.4125	2.6125	1.7375	3.675	2.975	2.6			
Packed Bed		2	4	2	3	3	3	4	4	4			
Monolithic		3	3	3	3	3	3	3	3	3			
Laminate		4	4	4	3	3	3	3	3	3			

Figure x: House of Quality

The first step of this process was to assign weights to all customer requirements based on their importance and then rank their correlation to each engineering requirement on a scale of 1 to 5. The weight was then applied to these scores to find the relative importance of each engineering requirement. Next target values were set for each of these engineering requirements. The benchmark sorbent bed designs were then ranked relative to the customer and engineering requirements on the bottom and right side of the diagram. Lastly the correlations between engineering requirements were determined in the roof of the house. This diagram concluded that elements such as sensors, a programmable logic controller, variable frequency drive, and vacuum pressure would be crucial to the design. This diagram is iterative and may change based on updated client needs.

3 Research Within Your Design Space

3.1 Benchmarking

Most existing DAC systems rely on a thermal moisture swing where water is heated to create vapor for the desorption and stripping processes. For our team design we will be relying on a vacuum moisture swing where vacuum pressures are used to boil water at room temperature. Vacuum pumps typically require less energy than heating elements which will allow for a more energy efficient design. The use of vacuum pumps in the DAC process is a newer concept and little benchmarking is available. Due to this we will use thermal moisture swing data as the best estimate of sub system performance.

The most important subsystem within our DAC system is the Sorbent Bed where the reaction occurs. The most common sorbent structures in existing processes are packed bed, fluidized bed, monolith and laminate. Both packed and fluidized beds consist of an open column full of small sorbent beads. In the packed bed the beads are packed between two screens allowing a flow to pass with great contact as well as great pressure drop. In a fluidized bed the velocity is fine tuned so that beads are suspended in the air, often described as an indoor skydiving effect. Alternatively, the monolith and laminate structure consist of intricate structures made from sorbents that allow flow to pass. The monolith is like a honey comb structure and the laminate is composed of many sheets layered on top of each other.

A vacuum pump is needed to bring the system to the pressures needed. The most common types of vacuum pumps are rotary vane, diaphragm, scroll, and liquid ring pumps. Choosing a pump type depends primarily on the target pumping speed, pressure, and pump-down time. Each of those types of pumps are ideal for different ranges of target parameters. It was found that rotary vane and scroll pumps are designed to pump within the target parameters of the vacuum moisture swing (about 1m/s and 1kpa).

Given that the system needs to be automated, an automations control is necessary. For control architecture, three options were considered: OPC UA, Matlab, and Matlab with Modbus. All three could work for the project, but have varying levels of complexity and reliability. Using a PC with Matlab to communicate with a PLC communicating over Modbus was chosen due to it's simplicity and reliability.

Standard KF vacuum fittings will be used to build the system, these are available in various shapes, sizes and connection types. Filters will also be placed at various locations in the system, these are available in many different mesh sizes. Lastly the water vapor must be separated from the CO2 before capture. This can be achieved through condensation from cooling or repressurizing, It can also be achieved using additional sorbents with different properties.

3.2 Literature Review

3.2.1 Sorbent Properties and 3D Printed Sorbents (Justin Patterson)

[1] AmberLite™ IRA900 Cl Ion Exchange Resin

This source was very helpful in describing the conditions that our sorbents will operate under. This includes temperature and pH ranges. Physical properties of the sorbents were also described, such as the density, swelling, range of size distribution, and approximate expansion of a bed of the sorbents when introduced to air flow that creates a fluidized bed structure.

[2] Moisture-Driven CO2 Pump for Direct Air Capture

This source is a paper published by Professor Wade, who is our customer. It describes the governing chemical equations relating to the operation of our DAC reactor. These equations helped the team understand the reactions and define the basic steps of our reactor. It also provided experimental data that described the amount of time it took for relative concentrations of CO2 and water to get absorbed by the sorbents which will be very useful in determining the amount of time each state needs when we are testing the rig after construction.

3.2.1.1 Current reactors for operating conditions, reaction run times, etc

[3] CO_2 Capture From Air in a Radial Flow Contactor: Batch or Continuous Operation?

This research paper highlights the CO2 concentration profiles for absorption experiments, which will help in learning the optimum run time. In addition, it showed acceptable velocity ranges for the input air/water vapor and how the reaction output changes because of it.

[4] Analysis of direct capture of CO2 from ambient air via steam-assisted temperature–vacuum swing adsorption

This paper includes schematics for basic reactor design and specific electrical/thermal energy compared to CO2 production graphs. The equations they used we will likely need to calculate our parameters for our reactor in the future. Temperature, humidity, pressure, concentration of CO2/H2O graphs were provided that correspond to each step of the cycle that are completed throughout the reaction.

3.2.1.2 3D printing sorbents

[5] Scaling up 3D printed hybrid sorbents towards (cost) effective post-combustion CO2 capture: A multiscale study

For this source, I mainly focused on how they made their sorbent paste so that they could print it using a 3D printer that will be very similar to ours. They used, “polyethyleneimine (PEI) and multiwalled carbon nanotubes (MWCNT) as the main components, and in addition, minor amounts of dispersant (UBE, and methylcellulose (MC) as a binder to make the paste printable.” They are using a carbon-based sorbent just like the activated charcoal that we will use so this should be a great help. It also talks about the ratio they used for each ingredient and how to mix them to ensure the correct properties.

[6] Investigating The Performance Of 3-D Printed Sorbents For Direct Air Capture Of CO2

This research paper describes the full set up needed to accurately print structures with these experimental materials, pump pressure for nozzle control, ratios for the slurry and test results. We will use this as a guide for when we are putting our system together, and optimizing the sorbent mixture and print quality.

[7] 3D-Printing of Adsorbents for Increased Productivity in Carbon Capture Applications (3D-CAPS)

This source is very similar to the source above, however, it focuses on silica based sorbents which is what our IRA900 sorbents are made of. This will be helpful if we want to either grind the sorbents up into powders and make a paste or integrate the beads into the 3D printing material. Isoreticular shapes were produced that are another way of porous structure that we may want to experiment with.

3.2.2 Vacuum Equipment (Randy Brierley)

3.2.2.1 Vacuum Pump Sizing

1- [8] 200pg document from a manufacturer, covering basic physics to how to quantify all aspects of vacuum

2- [9] A distributor website discussing the more qualitative aspects and overview

3.2.2.2 Vacuum Fittings

1- [10] A distributor website discussing the more qualitative aspects and overview
2- [11] A guide intended for technicians maintaining vacuum systems
3- [12] From a manufacturer of vacuum furnaces, covers resistance to gas flow in vacuum pipelines

3.2.2.3 Vacuum Standards

1- [13] From a manufacturer of vacuum furnaces, covers resistance to gas flow in vacuum pipelines
2- [14] Broad scope of engineering fundamentals, has a chapter on vacuum systems

3.2.3 Reactor Types (Elijah Woolridge)

3.2.3.1 Packed Bed

[15] Flow Through Packed Beds:

Describes the pressure drop across a packed bed and the use of the Ergun equation.

3.2.3.2 Fluidized bed

[16] 50 years of Geldart classification – ScienceDirect:

This is a state-of-the-art article describing the Geldart classification of fluidization behavior as well as key characteristics of each region. In the case of IRA900, the bed should exhibit type B fluidization as a sand like particle with bubbling, a low fluidization height, and immediate de-fluidization.

[17] Fluid Mechanics for Fluidized Beds:

Describes the pressure drop and critical velocities for fluidized beds. Provides equations for the terminal velocity of particles and the weight of a bed of particles.

[18] Aeration, fluidization, permeability of powders:

Defines the key behavior of a fluidized bed, namely the constant pressure drop and the expansion of the bed. It also provides visuals for pressure and volume at varying speeds.

[19] Comparison of Attrition Test Methods: ASTM standard fluidized bed vs jet cup | Industrial &

Engineering Chemistry Research:

Describes the increased wear on particles present in fluidized bed experiments and attempts at building on current endurance testing standards of particles. This will be a major deciding factor for the suitability of IRA 900 in fluidized beds.

3.2.3.3 Monolith and Laminate

[20] Systems design and economic analysis of direct air capture of CO2 through temperature vacuum swing adsorption using MIL-101(CR)-PEI-800 and mmen-mg2(dobpdc) MOF adsorbents | Industrial & Engineering Chemistry Research:

Describes the efficiency, cost, and performance of laminate and monolith structures for temperature swing sorbents. Much of the analysis holds for moisture swing processes.

[21] Friction modeling of flood flow simulations | Journal of Hydraulic Engineering | Vol 144, no 12

Defines a general approximation for the darcy friction factor for use in all flow regimes with a high degree of accuracy.

3.2.4 CFD Simulation and Validation (Branden Welker)

Throughout the design process, CFD will be used to simulate fluid flow through the sorbent structure. To better understand the modeling process a literature review was performed on the topic of CFD simulation and validation.

3.2.4.1 Flow Through Sorbent Beds

[22] [23] [24] These first three sources are very similar with slight differences in parameters geometry and sorbent type. All three sources are an overview of using ANSYS to model the capture of C02 passing through a sorbent bed. These sources provide boundary conditions and user defined functions that can be applied to our simulations. These sources also validated their data using experimental data. These sources will help to setup any CFD simulations performed

[25] This source provides some similar information to the previous sources with the addition of sorbent expansion. This includes the user defined function used to model the sorbent expansion as well as the variance in results it caused.

3.2.4.2 Flow Through Complex 3D printed Structures

[26] This source is an overview and comparison of modeling flow through packed beds and 3D printed structures. Some validation is provided for these 3D printed structures

[27] This source is a review of pressure drops across various sorbent structures based on CFD simulations. This provides a rough structure for performing these simulations and a process for optimizing this data.

3.2.4.3 CFD Validation

[28] This source is an overview of validation and verification of CFD simulations. This source introduced the standard (AIAA G-077-1998) which provides framework for validation and verification of CFD. The information is more related to aerospace, but many concepts can be applied to any simulation.

3.3 Mathematical Modeling

3.3.1 Sorbent Density, Volume and CO_2 capture capacity (Justin Patterson)

3.3.1.1 Sorbent Diameter and Mass Measurement

An experiment was set up using an environmental chamber that could control the concentration of water vapor in the air. This device was set to 95% humidity, and the sorbents were in the chamber for 2 hours. This was to ensure the sorbents had absorbed near the maximum amount they could absorb, and 2 hours would be a lot longer than a cycle we would run when the reactor is complete, so it was overkill. To determine the diameter of the sorbents, metal calipers were used. These calipers had an accuracy of ±.02mm. The scale that was used was in the environmental chamber that post doctorate research Golnaz uses to measure the capacity of the sorbents. The scale was accurate down to one micrometer, so it was more than enough for this application. Each sorbent bead was measured individually for diameter, and all of them were weighed at the same time.

3.3.1.2 Sorbent Volume and Density Calculation

After the data was collected, calculations were performed to obtain the average volume and total volume of all sorbents. Each sorbent volume was calculated individually using its respective diameter. These calculations were then averaged to determine the expansion and summed to determine the density for both wet and dry beads.

$$V = \left(\frac{4}{3}\right) * \pi * \left(\frac{D}{2}\right)^3$$

$$\frac{3.51\ mg}{3.03\ mm^3} = 1159\ \frac{kg}{m^3} \qquad \frac{4.87\ mg}{3.97\ mm^3} = 1227\ \frac{kg}{m^3}$$

3.3.1.3 CO_2 Capture Capacity

$$\left(\frac{mmol}{g}\right) CO_2 * g * \left(\frac{1\ mol}{1000\ mmol}\right) = mol\ CO_2$$

$$mol\ CO_2 * \left(\frac{g}{mol}\right) = g\ CO_2$$

$$\left(\frac{mmol}{g}\right) H_2O * g * \left(\frac{1\ mol}{1000\ mmol}\right) = mol\ H_2O$$

$$mol\ H_2O * \left(\frac{g}{mol}\right) = g\ H_2O$$

3.3.2 Major Head Loss (Branden Welker)

To determine the required pump parameters, we must calculate the total head loss or pressure drop across the system. To calculate head loss due to friction in straight sections of pipe the Darcy-Weisbach can be used [30].

$$h_{l,major} = f\frac{L}{D}\frac{V^2}{2g}$$

$h_{l,major}$ = major head loss (m)

f = Darcy friction factor

L = pipe length (m)

D = pipe diameter (m)

V = fluid velocity (m/s)

g = gravity (m/s^2)

Where $h_{l,major}$ is head loss caused by friction, f is the darcy friction factor, L is the length of pipe, D is the pipe diameter, V is the fluid velocity and g is gravity. To find the darcy friction factor Reynolds number must first be calculated with the following equation [30].

$$Re = \frac{\rho V D}{\mu}$$

Re = Reynolds number

ρ = Darcy friction factor (kg/m^3)

μ = Fluid viscosity (Pa*s)

For laminar flow (Re < 2300) the following can be used to find the darcy friction factor [30].

$$f = \frac{64}{Re}$$

Additionally, velocity and volumetric flow rates can be compared with the following [30].

$$\dot{Q} = A_c V$$

$\dot{Q}$ = volumetric flowrate (m^3/s)

A_c = cross-sectional area of pipe (m^2)

3.3.3 Packed and Fluidized Beds (Eli Woolridge)

The standard equation for the pressure drop across a packed bed is the Ergun equation. This is an important value to determine because it controls the behavior and efficiency of non-structured sorbent

beds, such as what will be used with the IRA900.

$$\frac{\Delta P}{L} = \frac{(150 \cdot \mu \cdot (1-\varepsilon)^2 \cdot U_0)}{\varepsilon^3 \cdot d^2} + \frac{(1.75 \cdot (1-\varepsilon) \cdot \rho \cdot U_0^2)}{\varepsilon^3 \cdot d}$$

$P =$ Pressure (kPa)

$L =$ Bed depth (m)

$\mu =$ Viscosity (kg/m*s)

$\varepsilon =$ Void fraction

$d =$ Particle diameter (m)

$U_0 =$ Superficial velocity (m/s)

A packed bed blown from below with no compression will begin to fluidize once the pressure drop across the bed becomes greater than the weight of the bed [17]. In this state the bed expands, and the void fraction increases until the Ergun equation is no longer greater than the weight of the bed. This state experiences excellent heat convection, low pressure drop, and good air contact at the cost of greater wear on the sorbent and lower bed density. The bed weight and fluidized pressure drop are calculated using the following formula.

$$\frac{\Delta P}{L} = g \cdot (\rho_s - \rho)$$

$g =$ Gravity = 9.81 (m/s^2)

$\rho_s =$ Particle density (kg/m^3)

$\rho_= $ Fluid density (kg/m^3)

Fluidization breaks when the drag on individual particles overcomes the weight of the particle [17]. This critical superficial velocity is equal to the terminal velocity of the particle. The equation to determine this varies based on the Reynolds number. These equations are as follows.

$$Re < 1 \quad \Longrightarrow \quad u_t = \frac{(\rho_s - \rho) \cdot g \cdot d^2}{18 \cdot \mu}$$

$$1 < Re < 500 \quad \Longrightarrow \quad u_t = \left[\frac{4 \cdot (\rho_s - \rho) \cdot g \cdot d}{3 \cdot \rho \cdot C_p}\right]^{\frac{1}{2}}$$

$$where\ C_p = \frac{18}{Re^{\frac{3}{5}}}$$

$$500 < Re < 2 \cdot 10^5 \quad \Longrightarrow \quad u_t = \left[\frac{3 \cdot (\rho_s - \rho) \cdot g \cdot d}{\rho}\right]^{\frac{1}{2}}$$

$u_t =$ Terminal velocity (m/s)

$d =$ Particle diameter (m)

3.3.4 Monolith and Laminate Structures (Eli Woolridge)

In most of the literature the Heigen-Poiseuille equation is used to determine the pressure drop across structured sorbents. This is generally considered to provide an overestimate and is suitable for most cases. The form of the equation changes slightly between monolith and laminate structures.

For laminate structures: $\frac{\Delta P}{L} = \frac{U_{in} \cdot 12 \cdot \mu}{h^3}$

For Monolith structures with square channel: $\frac{\Delta P}{L} = \frac{U_{in} \cdot 8 \cdot \pi \cdot \mu}{h^4}$

$h =$ Plane separation (m)

$U_{in} =$ Interstitial velocity (m/s)

The Heigen-Poiseuille equation is known to be inaccurate for fluids with particularly low viscosity such as low-pressure water vapor so it is supplemented with the Darcy-Weisbach Equation. In this case the extreme variations in Reynolds numbers within the channels make the previous darcy friction factor no longer suitable. Instead, the Bellos-Nalbantis-Tsakiris approximation is used as it is considered accurate through all flow domains [21].

$$f = \left(\frac{64}{Re}\right)^a \cdot \left[.75 \cdot \ln\left(\frac{Re}{5.37}\right)\right]^{2\cdot(a-1)\cdot b} \cdot \left[.88 \cdot \ln\left(3.41 \cdot \frac{h}{K_s}\right)\right]^{2\cdot(a-1)\cdot(1-b)}$$

where: $a = \frac{1}{1+\left(\frac{Re}{2712}\right)^{8.4}}$

$$b = \frac{1}{1+\left(\frac{Re}{150 \cdot \frac{h}{K_s}}\right)^{1.8}}$$

$K_s =$ Surface roughness (m)

$f =$ Darcy friction factor

3.3.5 Vacuum Pump (Randy Brierley)

A primary variable for sizing vacuum pumps is pumping speed. This depends on the effective pumping speed, which can be found by relating it to mass flow. In the case of this vacuum moisture swing device, the mass flow will be determined by the saturation temperature and the heat input to the water reservoir. The temperature and pressure are known, so only the heat input to the water reservoir is required to be chosen. From there, it can be calculated back to a pumping speed.

$$\dot{Q} = VIS_f$$

$$\dot{m}_v = \dot{Q}/h_{fg}(T)$$

$$\dot{m}_v = \rho_v S_{eff}$$

$$\rho_v = MP/R(T)$$

$$S_{eff} = S_{pump} C_{total}/(S_{pump} + C_{total})$$

$\dot{Q} = Power\ input$

$V = voltage$

$I = current$

$S_f = safety\ factor$

$\dot{m}_v = mass\ flow\ rate$

$h_{fg} = specific\ enthalpy$

$T = temperature$

$\rho_v = density$

$$S_{eff} = effective\ pumping\ speed$$

$$M = molar\ mass$$

$$P = Pressre$$

$$R = gas\ constant$$

$$S_{pump} = pumping\ speed$$

$$C_{total} = total\ conductance$$

3.3.6 Condensation Requirements (Branden Welker)

After vapor stripping has occurred the carbon dioxide water vapor mixture must be condensed so the liquid water can be separated from the carbon dioxide gas. If cooling is used for this process the required refrigeration can be found using the conservation of energy equation from the first law of thermodynamics [29].

$$\frac{dE}{dt} = \dot{Q} - \dot{W} + \sum_i \dot{m}_i \left(h_i + \frac{V_i^2}{2} + g z_i \right) - \sum_e \dot{m}_e \left(h_e + \frac{V_e^2}{2} + g z_e \right)$$

$E =$ total energy (W)

$\dot{Q} =$ Particle density (W)

$\dot{W} =$ Fluid density (W)

$\dot{m} =$ mass flowrate (kg/s)

$h =$ enthalpy (J/kg)

$V =$ fluid velocity (m/s)

$g =$ gravity (m/s^2)

$z =$ position in z direction (m)

i denotes inlet, e denotes exit

4 Design Concepts

4.1 Functional Decomposition

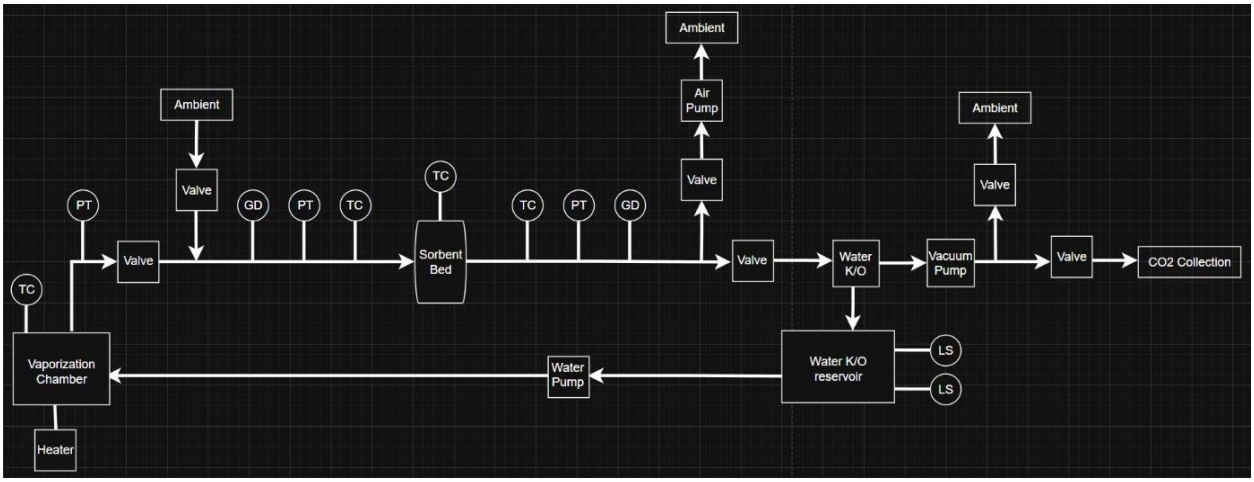

Figure x: Functional Decomposition of DAC System

Figure x shows the functional decomposition of the entire DAC system. TC represents thermocouples, PT represents pressure transducers, GD represents gas detectors and LS represents level sensors. An updated version based on design selection will be shown in 4.4 final design. The two main processes occurring in the sorbent bed and vaporization are represented by the black box diagrams below.

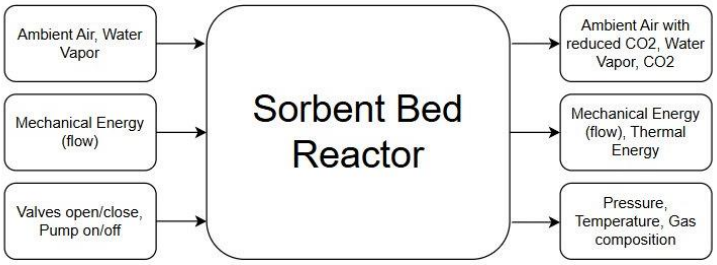

Figure x: Sorbent Bed Black Box Model

Figure x: Vaporization Chamber Black Box Model

4.2 Concept Generation

4.2.1 Valve Type (Eli Woolridge)

The type of valve used to isolate sections of the test rig plays a key role in the efficiency, safety, effectiveness, and ease of automation of the system. To minimize complexity, the valves should also interface with KF fittings and be electronically actuated. For this application, there are several types of valves that are commonly used and fit these characteristics. These being needle or gas dosing valves, butterfly valves, gate valves, globe valves, and ball valves. Each provide a unique combination of benefits and limitations.

4.2.2 Vapor CO2 Separation (Branden Welker)

During the vapor stripping stage of the cycle a mixture of water vapor and CO2 gas will leave the sorbent bed heading to the pump. To capture close to pure C02 this water must be separated from the C02 and recycled to the water reservoir. This separation can be achieved through pressurization, absorption, or cooling. For pressurization the water vapor would have to pass through the pump back to atmospheric pressure where it would condensate at room temp requiring no extra process. If absorption is chosen an additional sorbent bed featuring different sorbents must be added after the bed where the main reaction occurs. This would also require an additional process to then remove the water from these sorbents. Lastly for cooling, a refrigeration element would be required which would use additional energy, however, the water can then be knocked out before the pump. Since vacuum pressures are used it should be considered that liquid water does not exist below 0.6 kPa.

4.2.3 Pipe Diameter (Branden Welker)

Standard KF vacuum fittings and tubing will be used to construct most of the DAC system. These tubes will be used for their commercial availability and ability to withstand pressures significantly lower than the expected operating pressure. These tubes come in a large variety of diameters. The available options in our expected size range are KF16, KF25, KF40 and KF50 where the number represents the inner diameter in mm. These fittings and tubes can be attached using clamps and have a spot for a seal or filter between sections. There are many available fittings and adapters to connect valves, sensors and pumps. All components will be made of 3/16 stainless steel due to its corrosion resistance.

4.2.4 Control architecture (Randy Brierly)

A number of different control architectures would function for this project. The ones considered were OPC UA, Matlab, and Modbus with Matlab. OPC UA was ruled out due to it's complexity and having no one on the team with enough experience. OPC UA would be suitable for reliability and future expansion. Matlab alone would be too basic for future expansion, and less reliable. Modbus over a PLC to Matlab on a PC was chosen for this project. It will provide a reliable and relatively simple setup with the ability to expand.

4.2.5 Sorbent Mesh and Filters (Justin Patterson)

4.2.5.1 Sorbent Mesh

Our smallest measured particle size has a diameter of .35mm. To be safe, we want our mesh to be near .2mm in case for any other smaller particles, this corresponds to a mesh size of 70 (.21mm). We will use a

centering ring with this mesh integrated into it to keep the sorbent beads from leaving the reactor column.

4.2.5.2 Ambient Air and Pump Filters

The inlet ambient air filtration system will need 3 stages, with each one making the next filter in line more efficient and last longer. The pump filtration system doesn't need the largest filter due to the large filter on the ambient air. The HEPA filters are the industry standard for protecting sensitive equipment such as sensors. ULPA filters were decided against due to their vastly restricted airflow.

4.2.6 Vacuum Pump (Randy Brierly)

The vacuum pump is arguably the most important part of our system. It will be used to control the mass flow, internal pressure and to pull air in from outside the reactor. The three main types are diaphragm pumps, rotary vane pumps, and turbomolecular pumps. These pumps all increase with flow rate and have pros/cons regarding pressure drop, power usage and flow rate which will be discussed in section 4.3

4.2.7 Sorbent Structure (Eli Woolridge)

There are two major types of sorbent structure, these being structured and unstructured. The structured category is generally made of sheets or extruded ceramic and is defined by its ability to hold a distinct shape. The most common types to be considered are laminar and monolith type structures. A laminate structure is composed of parallel sheets of sorbent which the fluid passes between. Monolith structures contain many even channels through a block. Other shapes are possible but not common and difficult to simulate or fabricate. Unstructured sorbents often take the form of beads or powders. The standard bed configuration is a packed bed, though in rare cases a fluidized bed may be employed.

4.3 Concept Selection and Criteria

[Outline the selection criteria that was used for concept selection. These must be rooted in the engineering requirements and be quantifiable through calculations (for designed parts) and/or well-known specifications (for purchased parts). These calculation results and specifications MUST be summarized and discussed.]

4.3.1 Sorbent Properties (Justin Patterson)

4.3.1.1 Sorbent Volume and Density Calculation

$$\frac{3.51\ mg}{3.03\ mm^3} = 1159\ \frac{kg}{m^3} \qquad \frac{4.87\ mg}{3.97\ mm^3} = 1227\ \frac{kg}{m^3}$$

	Diameter (mm)	Volume (mm^3)	Density (kg/m^3)
Pre-Absorption (Dry)	0.568	0.1105	1227
Post-Absorption (Wet)	0.596	0.1212	1159

The wet beads achieved a 9.68% volume increase and a 5.87% density decrease. This was a lot less than our original estimates from Professor Wade and the specification sheet. This is also due to the ion exchange process that Golnaz puts them through to enable them to bond with CO2. By soaking them in a solution for days, there are lots of flakes that fall off, and the sorbents expand greatly. Knowing these facts and in talking with her, we believe that after this first expansion, the sorbents don't expand to their full size again because that extra volume sheds off.

4.3.1.2 CO_2 Capture Capacity

$$0.8\left(\frac{mmol}{g}\right)CO_2 * \ 100\ g\ * \left(\frac{1\ mol}{1000\ mmol}\right) = \ 0.08\ mol\ CO_2$$

$$0.08\ mol\ CO_2 * \ 44.01\left(\frac{g}{mol}\right) = \ 3.521\ g\ CO_2$$

$$30\left(\frac{mmol}{g}\right)H_2O * \ 100\ g\ * \left(\frac{1\ mol}{1000\ mmol}\right) = \ 3\ mol\ H_2O$$

$$3\ mol\ H_2O * \ 18.02\left(\frac{g}{mol}\right) = \ 54.06\ g\ H_2O$$

For 100g of sorbent it will need 54.06g of water to capture 3.521 g of CO2. Different sources provide values closer to 2 mmol/g CO_2 which would result in 8.8 grams of CO_2 captured per 100 grams of sorbent

4.3.2 Valve Type (Eli Woolridge)

Valve types were evaluated on a scale of –5 to 5 against relevant customer and engineering requirements with critical failures of –5, highlighted in red, eliminating a design.

Engineering Requirements	**2a. Minimize pressure drop**	**2b. Keep air velocity within 1m/s**	**3a. Vacuum pressure below 3 Kpa**	**6b. Incorporate control logic**	**Customer Requirement: Low Cost**	**Customer Requirement: Corrosion and abrasive resistance**	
Ball Valve	5	2	5	3	4	4	23
Butterfly Valve	5	5	-5	5	5	-2	13

Globe Valve	0	5	5	4	0	2	16
Needle	-5	4	5	5	5	1	19
Gate	5	2	5	4	-2	-1	13

This chart reveals that butterfly valves and needle valves are not suitable due to pressure requirements and pressure drop requirements, respectively. The best valve for our use case is ball valves. These are common in fluid applications but not often electronically actuated in vacuum systems. They are more often used as manual shutoff valves. As such, globe valves may be necessary to use due to part availability.

4.3.3 Vapor CO2 Separation (Branden Welker)

To determine the best way to separate water vapor from CO2 a pro-con list was created and assessed. This information can be seen below.

	Pros	Cons
Pressurization	No additional energy required No additional systems required	Water vapor may ruin pump
Absorption	Water knockout before pump	May require additional cycles May require additional energy Additional components required
Cooling	Water knockout before pump Easier freeze thaw to ensure maximum separation	Additional energy required Additional components required

Table x: Pros and Cons of water separation

Based on this data a final selection could not be made for the separation process. Absorption has been ruled out due to the extensive cons and minimal pros. If a pump can be found that allows water to pass through, pressurization will be selected. If a pump cannot be found, Cooling will be selected at the best option. Using the first law of thermodynamics, it was estimated that around 17W of refrigeration will be

required to cool the water to liquid state.

4.3.4 Pipe Diameter (Branden Welker)

The factors used to determine pipe selection can be seen below in table x. Head loss per unit length was calculated using the Darcy-Weisbach equation and shows us how much pressure is lost from friction at various diameters. The flowrate tells us how fast vapor can move through at a practical velocity of 0.75 m/s. increasing this will allow more vapor stripping but requires more pumping power. Lastly the sorbent size was compared to the pipe diameter to ensure a considerable difference in size so a scaled-up version would have more consistent results. 3D printer tolerances were also considered relative to pipe diameter.

Diameter (mm)	**16**	**25**	**40**	**50**
Head loss per unit length (Pa/m)	0.622	0.255	0.099	0.064
Flowrate (cm^3/s)	151	368	942	1473
Sorbent diameter / pipe diameter	0.036	0.023	0.014	0.011

Table x: Pipe Diameter Selection and Criteria

Based on this data the 40mm inner diameter KF40 tubing was selected for the final system. This size is reasonably large enough for testing complex prints and yielding similar results after being upscaled. The larger size additionally reduces head loss due to friction. KF50 wasn't selected as this would require much more performance from the vacuum pump.

4.3.5 Filters (Justin Patterson)

Sorbent Mesh

We will use a centering ring like this one that goes in between our pipe fittings to keep sorbent beads out of the pipes and inside the reactor column.

Ambient Air and Pump Filters

Filter Stage	*Micron Size*	*MERV Rating*	*Purpose for Ambient Air Filtration*	*Purpose for Pump Air Filtration*
Stage 1: Mesh Screens	*50 to 100+ microns*	*1–4*	*Captures the **largest particles** such as sand or coarse debris*	*Not needed*
Stage 2: Polyester or Cartridge Filter	*1 to 10 microns*	*8–11*	*Captures dust, pollen and mold. Key for **protecting lifespan** of the **final, more expensive filter***	*Will capture larger sorbent particles. These will be from possible breakdown due to water absorption.*
Stage 3: HEPA Filter	*0.3 microns*	*17–20*	***Removes 99.97%** of particles with **diameters of .3 microns**. Crucial for **protecting sensors and the vacuum pump***	*Will capture the finest particles generated by the rubbing of the sorbents in a fluidized bed*

4.3.6 Vacuum Pump (Randy Brierly)

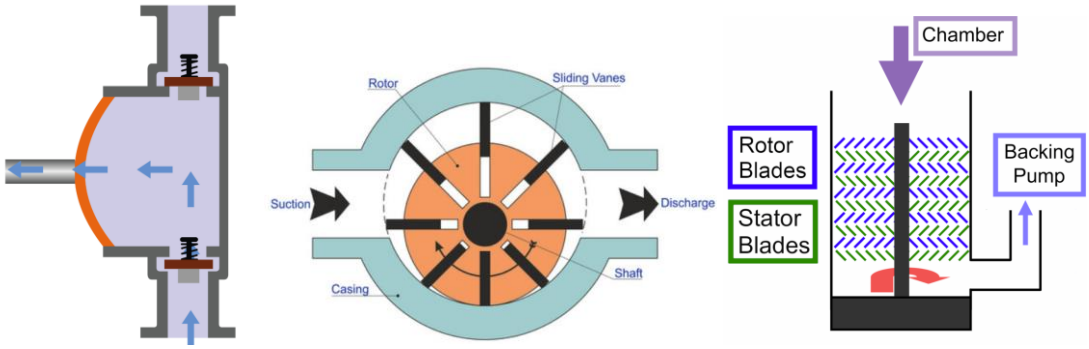

Vacuum Pump Types

- Diaphragm pump: 0.0017 – 0.1 L/s
- Rotary vane pump: 0.3 – 28 L/s
- Turbomolecular pump: 50 – 3000 L/s

Heating Element compared to flow rate of pump

$$S_{eff} = (S_{pump} * C_{total})/(S_{pump} + C_{total})$$

$$\dot{m}_v = \rho_v S_{eff} = (M_w P_{target})/(RT) * S_{eff}$$

$$m_v^{\dot{max}} = \dot{Q_{max}}/h_{fg}(T)$$

$$S_{eff} = \frac{RT}{M_w P_{target}} \dot{Q_{max}}/h_{fg}(T)$$

$$\mathrm{Q_{max}} = 120\mathrm{V} * 15\mathrm{a} * 0.8 = 1.44\mathrm{kW} = 1440\mathrm{J/s}$$

R=8.314 J/molK, Mw=0.018015 kg/mol, hfg=2.454E6 J/kg, T=293K, P=1000 Pa

S_{eff} = 0.079 m^3/s=79 L/s

Team evaluation proves that the rotary vane pump is best fit (next step is to talk with client about desired cycle time)

This S_{eff} is an upper max if a standard 120v outlet sized heating element is considered a max. Given the overly high flow rate, the conclusion here is that the heating element will not be a limiting factor.

4.3.7 Sorbent Structure (Eli Woolridge)

Using the equations previously described, MATLAB code found in appendix A was written. Additional dependencies can be found in appendix B and C. This code finds the pressure drop per unit length across

packed and fluidized beds for varying saturations and flow speeds. It also find the pressure drop per unit length across laminate and monolith structures for varying flow speeds and channel widths. Though all structures are expected to be tested, the expected performance can still be determined. Key plots are as follows.

4.3.7.1 Ergun Graphs

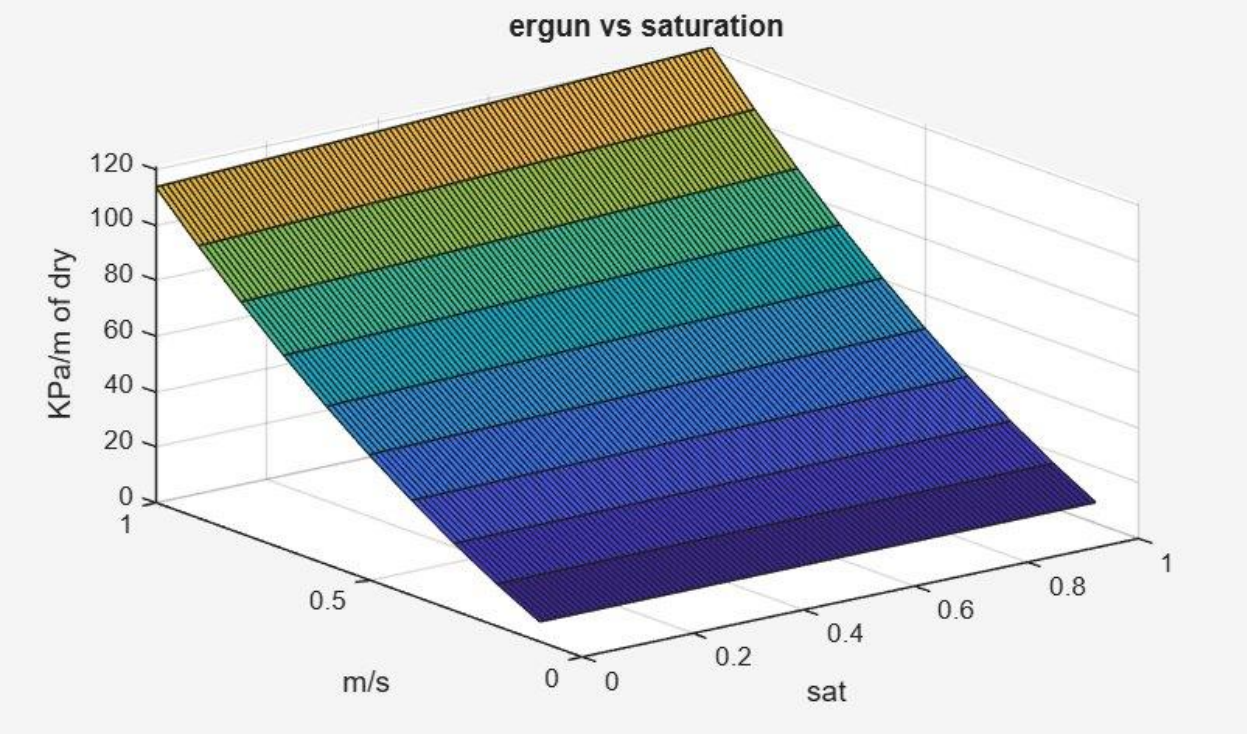

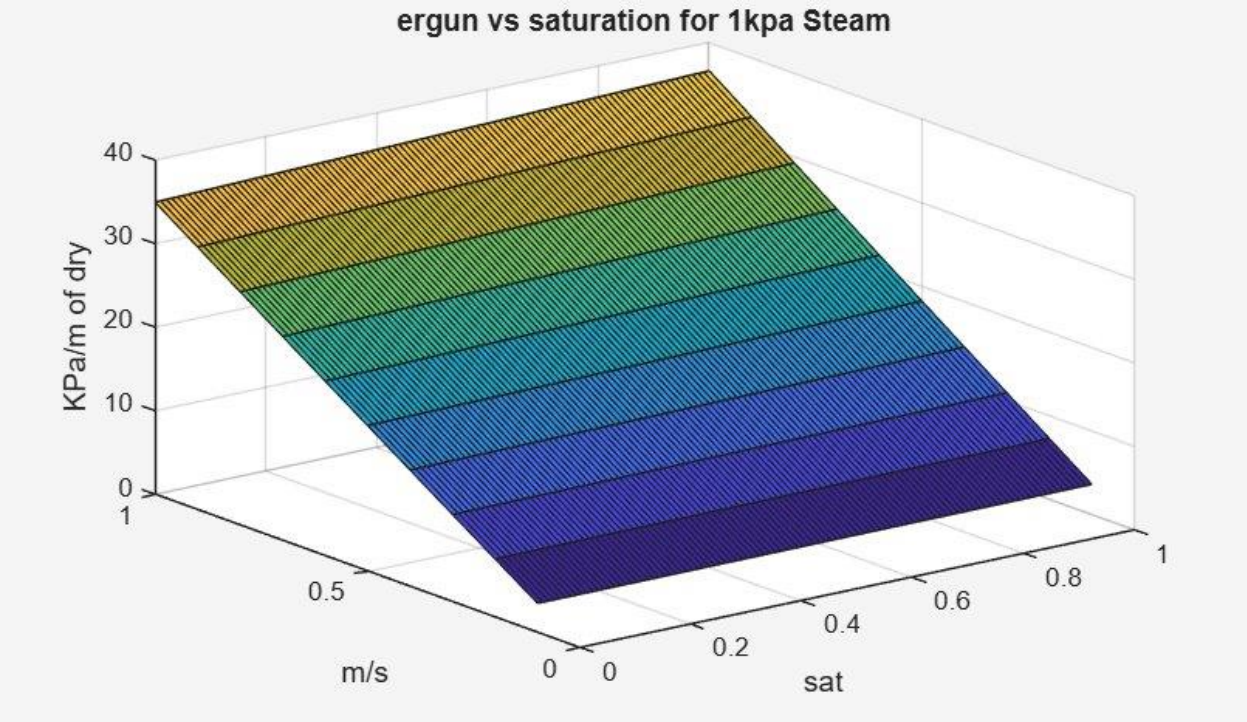

These graphs present a high-pressure drop but are balanced by exceptional sorbent capacity. They should perform well for this application.

4.3.7.2 Fluidized Bed

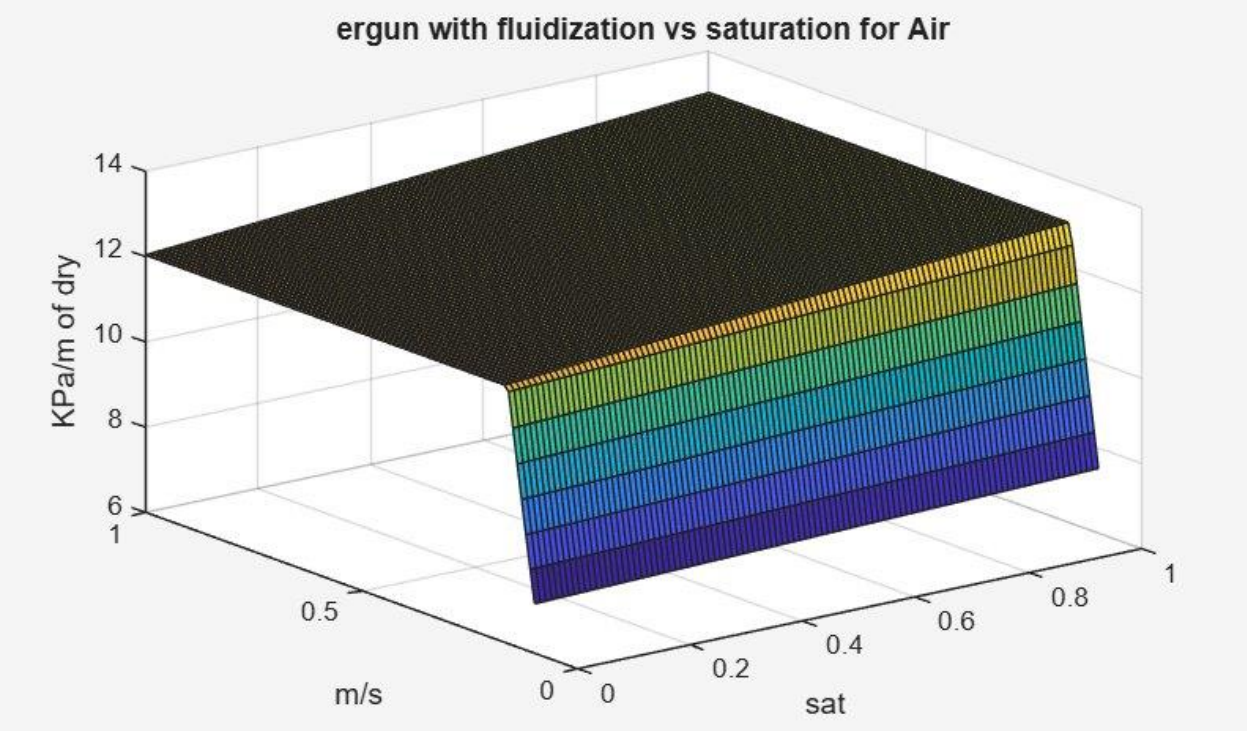

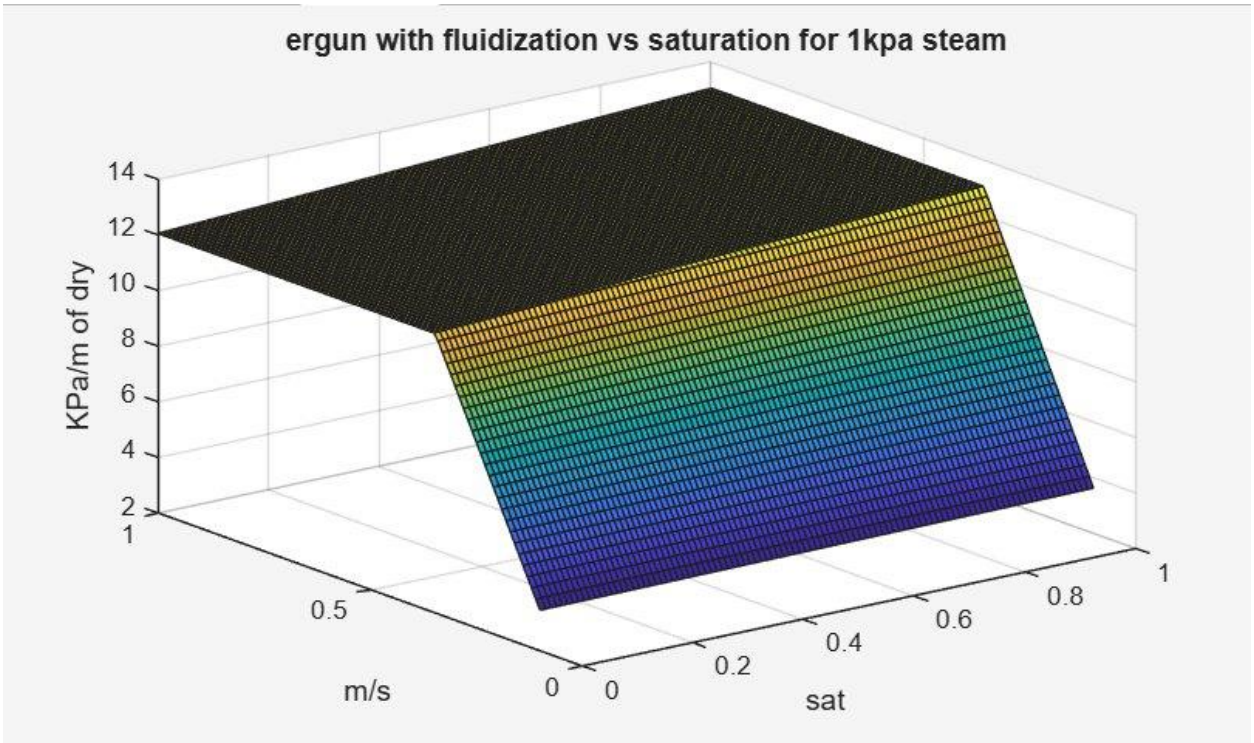

These show an excelent pressure drop and have a solid sorbent capacity. They should be our best option if sorbent degradation proves not to be an issue.

4.3.7.3 Monolith Structure

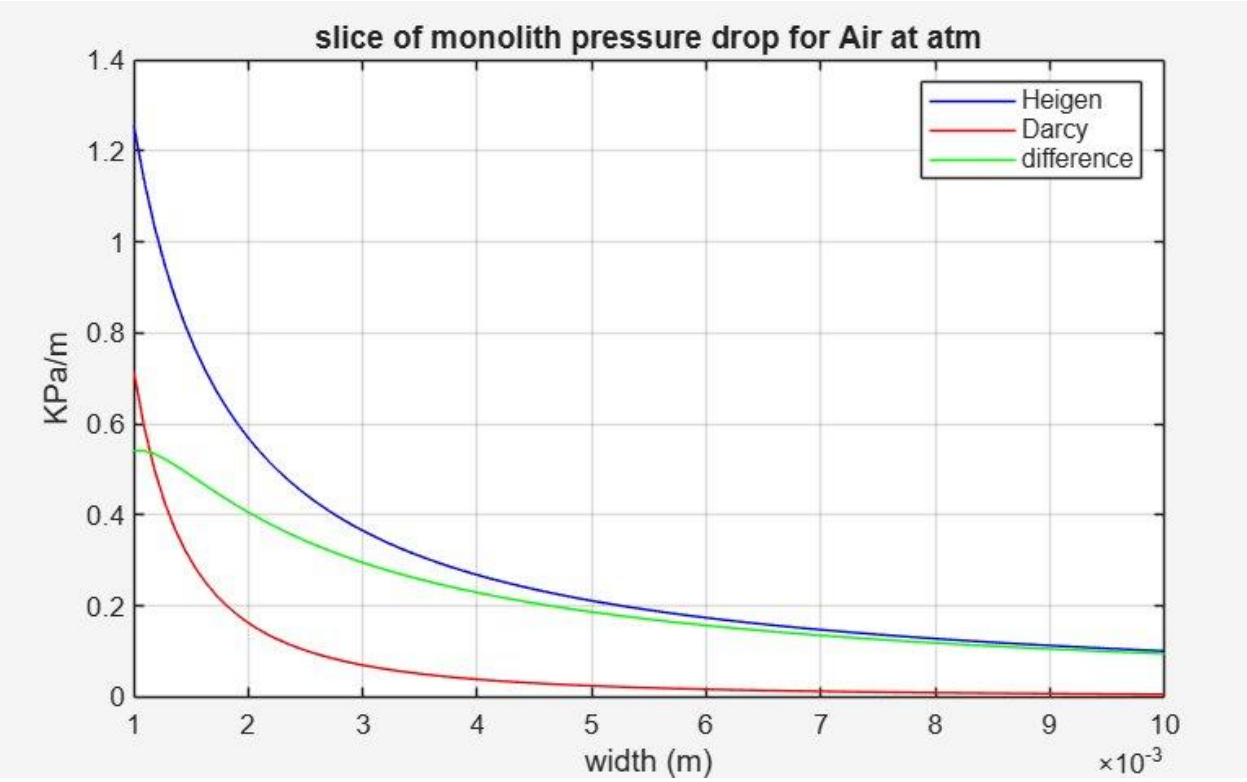

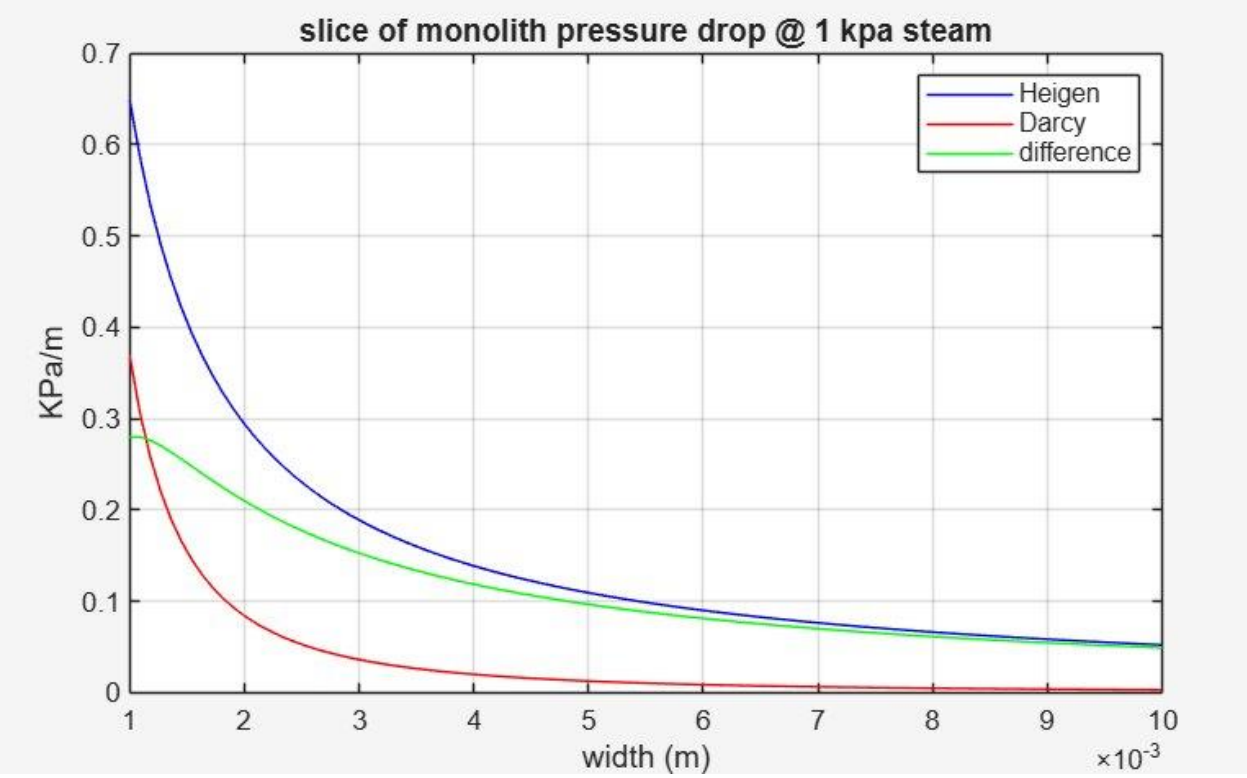

These show a very low pressure drop to balance a low sorbent capacity. They should be excelent for high flow rates but may still prove effective in this application.

4.3.7.4 Laminate structure

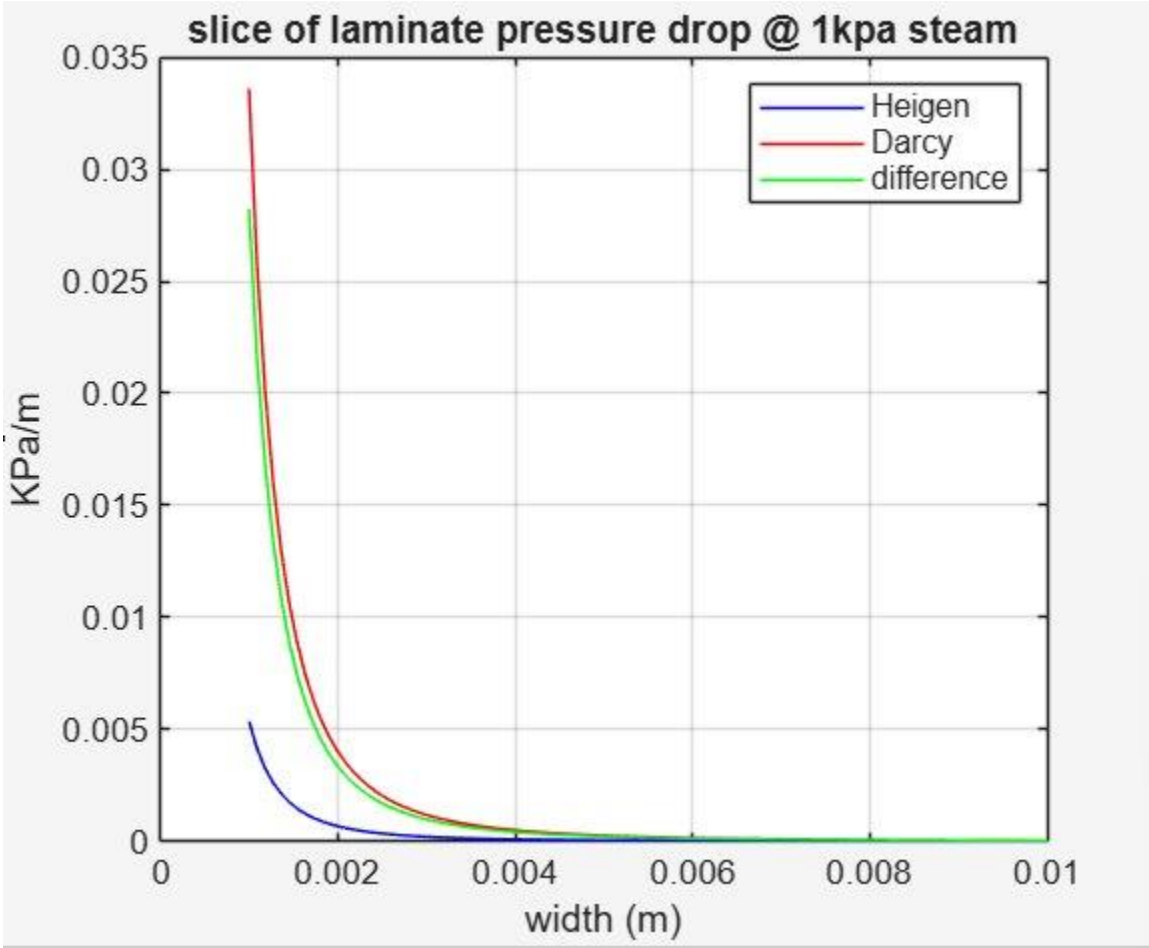

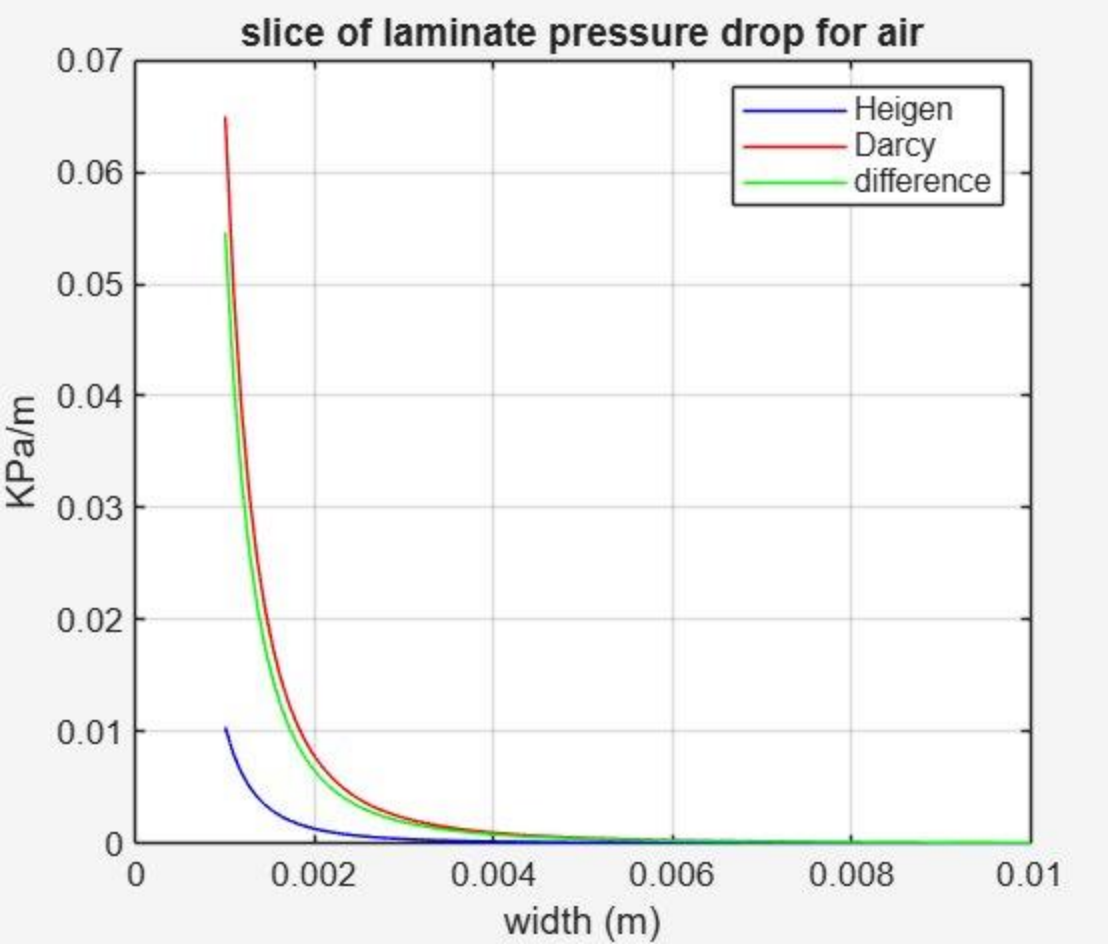

These show incredibly low pressure drop but at the cost of very low capacity. This is optimised for a different application.

4.4 Final Design

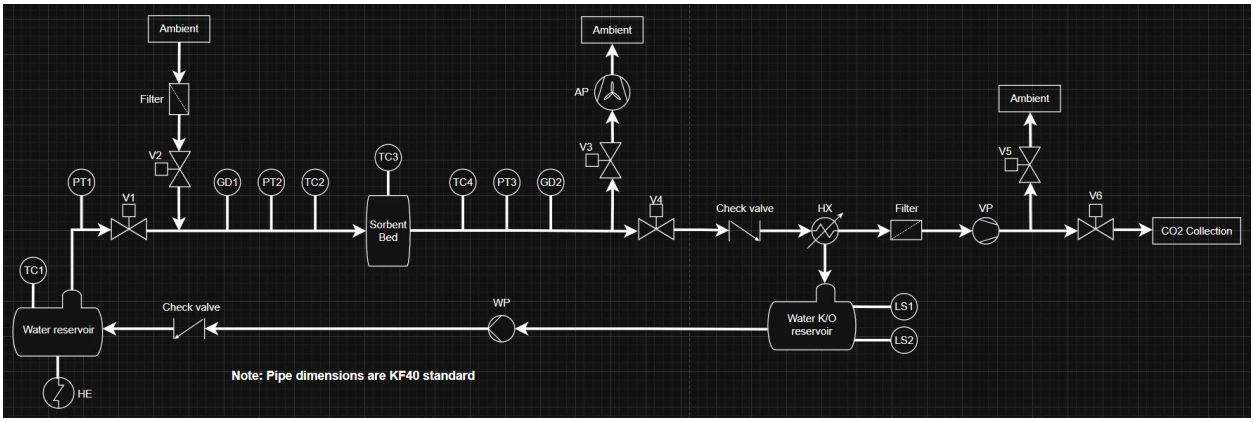

5 CONCLUSIONS

This project is working towards creating a direct air capture device that utilizes a vacuum moisture swing process to remove CO2 from air. Critical requirements of this project are to design efficient structured sorbent beds, create a functioning vacuum moisture swing device, and gather data from testing. The efficiency of the structured sorbent beds will be based on their performance compared the baseline of a packed sorbent bed. The structures will need to have a lower pressure drop than the packed bed, and ideally have comparable adsorption efficiency. The vacuum moisture swing device will need to be built with lab-grade parts and be fully automated, to allow long-term testing the Climate Solutions Lab. The device is required to function during testing of a variety of sorbent bed styles.

The proposed final solution is to build a device utilizing primarily KF40 vacuum fittings, electrically actuated valves, and a vacuum pump for the vacuum chamber. Ambient air will be pushed in by a blower fan. The water vapor will be knocked out by a heat exchanger, and a water capture reservoir with level sensors will trigger a water pump to refill the vaporization reservoir. Pressure transducers, thermocouples, and gas detectors, will provide data from testing. A control architecture of a PLC connected to a PC with Matlab, communicating over Modbus, will allow the system to be automated.

A special ceramic 3D printer will be used to print different structured sorbent beds. Utilizing ANSYS software, different structure designs will be evaluated and optimized. Once structures are selected, they will be 3D printed and used in testing in the vacuum moisture swing device.

6 REFERENCES

[1] 2019, "AmberLiteTM IRA900 Cl Ion Exchange Resin Gaussian, Macroporous, Strong Base Anion Exchange Resin for Industrial Demineralization Applications."

[2] Wade, J. L., Lopez Marques, H., Wang, W., Flory, J., and Freeman, B., 2023, "Moisture-d riven CO2 pump for Direct Air Capture," Journal of Membrane Science, **685**, p. 121954.

[3] Schellevis, M., Jacobs, T., and Brilman, W., 2020, "CO2 capture from air in a radial flow contactor: Batch or continuous operation?," Frontiers in Chemical Engineering, **2**.

[4] Stampi-Bombelli, V., van der Spek, M., and Mazzotti, M., 2020, "Analysis of direct capture of $${\hbox {CO}}_{2}$$ from ambient air via steam-assisted temperature–vacuum swing adsorption," Adsorption, **26**(7), pp. 1183–1197.

[5] Krishnamurthy, S., Roelant, R., Blom, R., Arstad, B., Li, Z., Rombouts, M., Middelkoop, V., Borras, A. B., and Naldoni, L., 2024, "Scaling up 3D printed hybrid sorbents towards (cost) effective post-combustion CO2 Capture: A multiscale study," International Journal of Greenhouse Gas Control, **132**, p. 104069.

[6] Obeng-Ampomah, T., 2020, "Investigating The Performance Of 3-D Printed Sorbents For Direct Air Capture Of CO2 by Terry Obeng-Ampomah."

[7] Sluijter, S., Boon, J., James, J., Krishnamurthy, S., Lind, A., Andreassen, K. A., Blom, R., Cormos, A. M., Sandu, V., and de Boer, R., 2021, "3D-printing of adsorbents for increased productivity in carbon capture applications (3D-caps)," SSRN Electronic

[8] Leybold Oerlikon Vacuum, 2015, *Flanges and Fittings (ISO-KF, ISO-K, ISO-F, CF) Catalog Part CP_080, Full Line Catalog 2015/2016*, Oerlikon Leybold Vacuum,

Frankfurt. Available at: CP_080_EN_T_809-882_Flange_and_Fittings.pdf (accessed Sept. 15, 2025).

[9] Umrath, W., Adam, H., Bolz, A., Boy, H., Dohmen, H., Gogol, K., Jorisch, W., Mönning, W., Mundinger, H.-J., Otten, H.-D., Scheer, W., Seiger, H., Schwarz, W.,

Stepputat, K., Urban, D., Wirtzfeld, H.-J.,and Zenker, H.-J., 2007, *Fundamentals of Vacuum Technology*, Oerlikon Leybold Vacuum, Cologne. Available at:

GrundlagenE (accessed Sept. 15, 2025).

[10] Hata, D. M., Brewer, E. V., and Louwagie, N. J., 2025, *Introduction to Vacuum Technology*, Milne Open Textbooks, State University of New York at Geneseo, Geneseo, NY.

Available at:Introduction to Vacuum Technology – Simple Book Publishing (accessed Sept. 15, 2025).

[11] Ruff, M., 2025, "A Guide to Vacuum Pump Sizing," *Blower & Vacuum Best Practices*. Available at: A Guide to Vacuum Pump Sizing | Blower & Vacuum Best

Practices (accessed Sept. 15, 2025).

[12] VTech Process Equipment, LLC, n.d., *Sizing Vacuum Pumps*, ThomasNet, Alpharetta, GA. Available at: Sizing Vacuum Pumps (accessed Sept. 15, 2025).

[13] Hicks, T. G., 2006, *Handbook of Mechanical Engineering Calculations*, 2nd ed., McGraw-Hill, New York.

[14] VAC AERO International, 2013, "Conductance & Throughput in Vacuum Pipelines," *VAC Aero*.

Available at: Conductance & Throughput in Vacuum Pipelines (accessed Sept.15, 2025).

[15] D. Thornhill, "Flow Through Packed Beds," Packed beds, . https://faculty.washington.edu/finlayso/Fluidized_Bed/FBR_Fluid_Mech/packed_beds_fbr.htm#ergun . (accessed Oct. 9, 2025).

[16] R. Cocco and J. W. Chew, "50 years of Geldart classification - sciencedirect," 50 years of Geldart classification, https://www.sciencedirect.com/science/article/pii/S0032591023006459 (accessed Oct. 9, 2025).

[17] D. Thornhill, "Fluid Mechanics for Fluidized Beds," FBR Fluid Mechanics, https://faculty.washington.edu/finlayso/Fluidized_Bed/FBR_Fluid_Mech/fluid_bed_scroll.htm (accessed Oct. 9, 2025).

[18] Www.powderprocess.net, "Aeration, fluidization, permeability of powders," Fluidization, Aeration, Permeability of powders : An overview, https://powderprocess.net/Powder_Flow/Aeration_Permeability.html (accessed Oct. 21, 2025).

[19] R. Zhao, J. G. Goodwin, K. Jothimurugesan, J. Spivey, and S. K. Gangwal, "Comparison of Attrition Test Methods: ASTM standard fluidized bed vs jet cup | Industrial & Engineering Chemistry Research," Comparison of Attrition Test Methods: ASTM Standard Fluidized Bed vs Jet Cup, https://pubs.acs.org/doi/10.1021/ie990730j (accessed Oct. 22, 2025).

[20] A. Sinha, L. Darunte, C. Jones, M. Realff, and Y. Kawajiri, "Systems design and economic analysis of direct air capture of CO2 through temperature vacuum swing adsorption using MIL-101(CR)-PEI-800 and mmen-mg2(dobpdc) MOF adsorbents | Industrial & Engineering Chemistry Research," Systems Design and Economic Analysis of Direct Air Capture of CO2 through Temperature Vacuum Swing Adsorption Using MIL-101(Cr)-PEI-800 and mmen-Mg2(dobpdc) MOF Adsorbents, https://pubs.acs.org/doi/10.1021/acs.iecr.6b03887 (accessed Oct. 9, 2025).

[21] V. Bellos, I. Nalbantis, and G. Tsakiris , "Friction modeling of flood flow simulations | Journal of Hydraulic Engineering | Vol 144, no 12," ASCE library, https://ascelibrary.org/doi/10.1061/%28ASCE%29HY.1943-7900.0001540 (accessed Oct. 9, 2025)

[22] N. A. A. Qasem and R. Ben-Mansour, "Energy and productivity efficient vacuum pressure swing adsorption process to separate CO_2 from CO_2/N_2 mixture using Mg-MOF-74: A CFD simulation," *Applied Energy*, vol. 209, pp. 190-202, Jan. 2018.

[23] Q. Chen, F. Rosner, A. Rao, S. Samuelsen, A. Jayaraman, and G. Alptekin, "Simulation of elevated temperature solid sorbent CO2 capture for pre-combustion applications using computational fluid dynamics," *Applied Energy*, vol. 239, pp. 374–387, Apr. 2019. doi: 10.1016/j.apenergy.2019.01.179

[24] E. S. Mogire, A. J. Mboya, E. E. Bakit, P. M. Musembi, M. Bwondera, D. K. Githinji, and V. V. Barasa, "Simulation and airflow experimentation of a multi-layer adsorbent chamber for enhanced direct air capture efficiency," in *Proc. 2024 Sustainable Research and Innovation Conf.*, JKUAT Main Campus, Kenya, Oct. 2–3, 2024, pp. 14–17

[25] E. Abbasi, A. Hassanzadeh, and J. Abbasian, "Regenerable MgO-based sorbent for high temperature CO_2 removal from syngas: 2. Two-zone variable diffusivity shrinking core model with expanding product layer," *Fuel*, vol. 105, pp. 128–134, Jan. 2013, doi: 10.1016/j.fuel.2012.06.005.

[26] A. M. Elkissi, F. Rezaei, and R. Smith, "Vacuum swing adsorption process for post-combustion carbon capture with 3D printed sorbents: Quantifying the improvement in productivity and specific energy over a packed bed system through process simulation and optimization," *Chemical Engineering Science*, vol. 253, p. 117585, May 2022. doi: 10.1016/j.ces.2022.117585

[27] S. Sluijter, J. Boon, J. James, S. Krishnamurthy, A. Lind, R. Blom, K. Andreassen, A. Cormos, V. Sandu and R. de Boer, "3D-printing of adsorbents for increased productivity in carbon capture applications (3D-CAPS)," *International Journal of Greenhouse Gas Control*, vol. 112, p. 103512, 2021. doi: 10.1016/j.ijggc.2021.103512.

[28] F. Stern, R. Wilson, and J. Shao, "Quantitative V&V of CFD simulations and certification of CFD codes," *International Journal for Numerical Methods in Fluids*, vol. 50, no. 11, pp. 1335-1355, 2006.

[29] M. J. Moran, H. N. Shapiro, D. D. Boettner, and M. B. Bailey, Fundamentals of Engineering Thermodynamics, 8th ed. Hoboken, NJ, USA: Wiley, 2015

[30] P. J. Pritchard, Fox and McDonald's Introduction to Fluid Mechanics, 10th ed. Hoboken, NJ, USA: John Wiley & Sons, 2019

7 APPENDICES

7.1 Appendix A: Variable_fluidized_calcs.m: The driver

```
clear all, close all
Uslice=1; % m/s The slice taken for the 2d graphs
Pslice=.01; % bar
Pcheck=.01; %pressure(bar) The pressure used in the 3d steam graphs
sat=linspace(1,0,101); %percent saturation of the beads
fluid=1; %1=steam, 2=air(pressure locked at 1bar)
E=.37; %voidfraction
if fluid==1
disp("steam")
else
disp("Air");
end
threede=[]; %initializing counters
u=[];
missed_Ps=[];
erg=[];
Heigen=[];
Darcy=[];
% Varies U and P to allow for 3D plotting
for U=.1:.01:1 % (m/s)
u=[u,U];%counts the U for the 3d graph
for P=.01:.01:1 %the last value here goes to the 3d plot (bar)
% Determines the dependent variables for the fluid
if fluid == 1
T=XSteam('TSat_p',P); %temp in deg C
p_fl=XSteam('rhoV_p',P); %fluid density(kg/m^3)
y=XSteam('my_pT',P,T+.1); %dynamic viscosity of fluid (pa*s) %function doesnt work on
the transition line so T is bumped
tolow=isnan(y);
if tolow==1 % x steam doesnt quite go lower than this for y so its a near
approximation
T=XSteam('TSat_p',.0153);
y=XSteam('my_pT',.0153,T+.1);
missed_Ps=[missed_Ps,P];
end
else
T=20; %temp in deg C
p_fl=1.225; %fluid density (kg/m^3)
y=.00001846; %dynamic viscosity of fluid (pa*s)
end
% determines dependent variables for the particle
d= @(sat) (.000596-.0005694)*(sat)+.0005694; %particle diameter (m)
p_par= @(sat) (1158.7-1227.3)*(sat)+1227.3; %particle density (kg/m^3)
d=d(sat);
p_par=p_par(sat);
V_per1m3dry= (d./.0005694).^3; %(vwet/vdry)
% calculates the pressure drops for key behaviors
%packed bed
```

```
dP = ergun(y,E,U,d,p_fl); %make sure input units are correct (Pa/m)
dP = dP/1000; %converts to (kPa/m)
%fluidization point
BedWeight= 9.81*(p_par-p_fl*ones(size(sat)))/1000; %downward pressure of the bed
(kpa/m)
%critical U point (i am aware the method is wierd)
Re=(p_fl*U*d)/y;
laminar= Re<=1;
Ucrit_lam=((p_par-p_fl*ones(size(sat)))*9.81.*d.^2)/(18*y);
transitioning= (Re>1) & (Re<500);
Cp=18./(Re.^(3/5));
Ucrit_tran=((4*(p_par-
p_fl*ones(size(sat)))*9.81.*d)./(3*p_fl*ones(size(sat)).*Cp)).^(1/2);
turbulent= Re>=500 ;
Ucrit_turb=((3*(p_par-p_fl*ones(size(sat)))*9.81.*d)./(p_fl*ones(size(sat)))).^(1/2);
Ucrit=laminar.*Ucrit_lam+transitioning.*Ucrit_tran+turbulent.*Ucrit_turb;
% determines which behavior is active and records its pressure drop
fluidized= BedWeight<dP & (U<Ucrit);
packed= BedWeight>=dP & (U<Ucrit);
flying= U>=Ucrit;
presspath= (packed.*dP)+(fluidized.*BedWeight) +(flying.*dP); %tracks which wins
%normalize all by bed height change
dP=dP.*V_per1m3dry;
presspath=presspath.*V_per1m3dry;
BedWeight=BedWeight.*V_per1m3dry;
%these ones are for monolyth structures
% constant wall thickness varried passage width
TH=.0001;%wall thickness
sqe=.001*ones(size(sat))+(sat.*.009) ;%varies edge of square passage from 1mm to 1cm
Ar=(sqe.^2)./((TH*ones(size(sat))+sqe).^2) ;%percent open space in channel cross
section assuming a wall thickness TH and a square edge sqe
Uint=U./Ar ;% flow speed in channels
R=sqe./2 ;%equivalent hydraulic radius of square passage
Reint=(p_fl.*Uint.*d)./y; %used for darcy friction factor fd
Heigenslice=(8*y.*Uint)./(R.^2) ; % pa/m Heigen-poiseuille equasion breaks down in
low viscosity
Heigenslice=Heigenslice/1000; % kpa/m
Arlam=(sqe.^2)./((TH*ones(size(sat))+sqe).*(TH*ones(size(sat)))) ;%percent open space
in laminate cross section assuming a wall thickness TH and a square edge sqe
Uintlam=U./Arlam ;% flow speed in channels
Heigenslicelam=(8*y.*Uintlam)./(R.^2) ; % pa/m Heigen-poiseuille equasion breaks down
in low viscosity
Heigenslicelam=Heigenslicelam/1000; % kpa/m
Esur=.05; %mm
Esur=Esur/1000; % surface roughness in m (used new sheet metal in table for .05 mm)
Afd=1./(ones(size(Reint))+(Reint./2712).^8.4);
Bfd=1./(ones(size(Reint))+(Reint./(150.*(2.*R/Esur))).^1.8);
% Darcy friction factor calculation on vector Reint using
% Bellos-Nalbantis-Tsakiris approximation
fd =(64./Reint).^(Afd).*(.75*log(Reint./5.37)).^(2.*(Afd-
ones(size(Afd))).*Bfd).*(.88.*log(3.41.*(2.*R)./Esur)).^(2.*(Afd-
ones(size(Afd))).*(ones(size(Bfd))-Bfd)) ;
```

```
Darcyslice=(fd).*(p_fl/2).*((Uint).^2)./(2.*R); % pa/m Darcy-Weisbach equasion
considered more accurate
Darcyslice=Darcyslice/1000 ; % kpa/m
Darcyslicelam=(fd).*(p_fl/2).*((Uintlam).^2)./(2.*R); % pa/m Darcy-Weisbach equasion
considered more accurate
Darcyslicelam=Darcyslicelam/1000 ; % kpa/m
% selects a slice of the 3d for a 2d graph
if U==Uslice & P==Pslice
figure(1)
xlabel('Saturation (%)');
ylabel('Pressure Drop (kPa/m of dry)');
title('Pressure Drop vs. Saturation');
grid on;
hold on;
plot(sat,BedWeight,'r');
plot(sat,dP,'g')
plot(sat,presspath,'b');
legend('Bed Weight','Ergun','Fluidized')
figure(7)
plot(sqe,Darcyslice,'b')
hold on
grid on
plot(sqe,Heigenslice,'r')
plot(sqe,Darcyslice-Heigenslice,'g')
title('slice of monolith pressure drop')
xlabel("width (m)")
ylabel("KPa/m")
legend('Heigen','Darcy','difference')
figure(8)
plot(sqe,Darcyslicelam,'b')
hold on
grid on
plot(sqe,Heigenslicelam,'r')
plot(sqe,abs(Darcyslicelam-Heigenslicelam),'g')
title('slice of laminate pressure drop')
xlabel("width (m)")
ylabel("KPa/m")
legend('Heigen','Darcy','difference')
end
if P==Pcheck
threede=[threede;presspath]; %records data for the set Pvalue
erg=[erg;dP];
Heigen=[Heigen;Heigenslice];
Darcy=[Darcy;Darcyslice];
end
end %for pressure
end %for velocity
hold off
% graphs all data in a 3d graph
figure(2)
surf(sat,u,threede)
title('ergun with fluidization vs saturation')
```

```
xlabel("sat")
ylabel("m/s")
zlabel("KPa/m of dry")
figure(3)
surf(sat,u,erg)
title('ergun vs saturation')
xlabel("sat")
ylabel("m/s")
zlabel("KPa/m of dry")
figure(4)
plot(sat,V_per1m3dry)
title('volume for constant # beads')
xlabel('sat')
ylabel('volume/volume dry (m^3)')
figure(5)
surf(sqe,u,Heigen)
title('Heigen-poiseuille vs cell width')
xlabel("width (m)")
ylabel("m/s")
zlabel("KPa/m")
figure(6)
surf(sqe,u,Darcy)
title('Darcy-Weisbach vs cell width')
xlabel("width (m)")
ylabel("m/s")
zlabel("KPa/m")
if length(missed_Ps)>0
message=['had to approximate P<.0153 to .0153 ',num2str(length(missed_Ps)),' times
due to data limitations, see missed_Ps for more info'];
disp(message)
end
```

7.2 Appendix B: Ergun.m : applies Ergun equation

```
%ergun Equasion dp/L
function [dPpL]=ergun(y,E,U,d,p)
% y= dynamic viscosity of fluid (pa*m)
% E= voidfraction (decimal)
% U= velocity of fluid (m/s)
% d= particle diameter (m)
% p= fluid density (kg/m^3)
% dPpl= change in pressure per length (Pa/m)
dPpL = (150.*y.*(1-E).^(2).*U)./(E^(3).*d.^2) + (1.75.*(1-E).*p.*U.^2)./(E.^3.*d);
```

7.3 Appendix C: Additional dependencies of variable_fluidized_calcs.m

- XSteam.m
    - Magnus Holmgren (2025). X Steam, Thermodynamic properties of water and steam. (https://www.mathworks.com/matlabcentral/fileexchange/9817-x-steam-thermodynamic-properties-of-water-and-steam), MATLAB Central File Exchange.

Retrieved October 20, 2025.